

# Procedural Texturing of Solid Wood with Knots

MARIA LARSSON, The University of Tokyo, Japan  
TAKASHI IJIRI, Shibaura Institute of Technology, Japan  
HIRONORI YOSHIDA, Future University Hakodate, Japan  
JOHANNES A. J. HUBER, Luleå University of Technology, Sweden  
MAGNUS FREDRIKSSON, Luleå University of Technology, Sweden  
OLOF BROMAN, Luleå University of Technology, Sweden  
TAKEO IGARASHI, The University of Tokyo, Japan

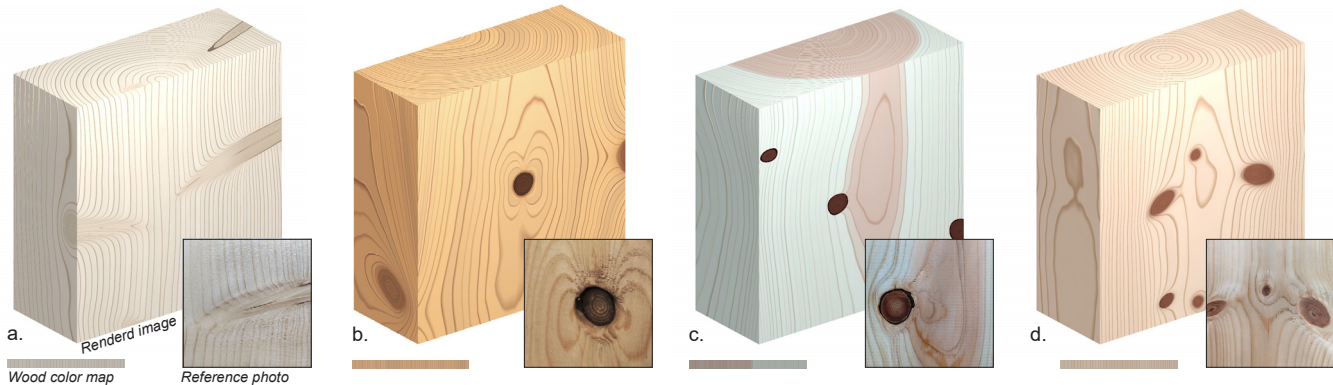


Fig. 1. Rendered images aimed at reproducing the annual ring patterns observed in the reference photographs, created using our procedural framework for texturing knotted wood. Each  $1200 \times 1200$  pixel sized image was rendered within 0.5 s, based on 600 KB color and geometry data.

We present a procedural framework for modeling the annual ring pattern of solid wood with knots. Although wood texturing is a well-studied topic, there have been few previous attempts at modeling knots inside the wood texture. Our method takes the skeletal structure of a tree log as input and produces a three-dimensional scalar field representing the time of added growth, which defines the volumetric annual ring pattern. First, separate fields are computed around each strand of the skeleton, i.e., the stem and each knot. The strands are then merged into a single field using smooth minimums. We further suggest techniques for controlling the smooth minimum to adjust the balance of smoothness and reproduce the distortion effects observed around dead knots. Our method is implemented as a shader program running on a GPU with computation times of approximately 0.5 s per image and an input data size of 600 KB. We present rendered images of solid wood from pine and spruce as well as plywood and cross-laminated timber (CLT). Our results were evaluated by wood experts, who confirmed the plausibility of the rendered annual ring patterns.

Link to code: [https://github.com/marialarsson/procedural\\_knots](https://github.com/marialarsson/procedural_knots).

Authors' addresses: Maria Larsson, The University of Tokyo, Japan, [ma.ka.larsson@gmail.com](mailto:ma.ka.larsson@gmail.com); Takashi Ijiri, Shibaura Institute of Technology, Japan, [takashi.ijiri@riken.jp](mailto:takashi.ijiri@riken.jp); Hironori Yoshida, Future University Hakodate, Japan, [hyoshida@hy-ma.com](mailto:hyoshida@hy-ma.com); Johannes A. J. Huber, Luleå University of Technology, Sweden, [johannes.huber@ltu.se](mailto:johannes.huber@ltu.se); Magnus Fredriksson, Luleå University of Technology, Sweden, [magnus.1.fredriksson@ltu.se](mailto:magnus.1.fredriksson@ltu.se); Olof Broman, Luleå University of Technology, Sweden, [olof.broman@ltu.se](mailto:olof.broman@ltu.se); Takeo Igarashi, The University of Tokyo, Japan, [takeo@acm.org](mailto:takeo@acm.org).

© 2022 Copyright held by the owner/author(s). Publication rights licensed to ACM. This is the author's version of the work. It is posted here for your personal use. Not for redistribution. The definitive Version of Record was published in *ACM Transactions on Graphics*, <https://doi.org/10.1145/3528223.3530081>.

CCS Concepts: • **Computing methodologies** → **Volumetric models; Texturing**.

Additional Key Words and Phrases: procedural texturing, volumetric texturing, natural phenomena, wood, smooth minimum, distance field

## ACM Reference Format:

Maria Larsson, Takashi Ijiri, Hironori Yoshida, Johannes A. J. Huber, Magnus Fredriksson, Olof Broman, and Takeo Igarashi. 2022. Procedural Texturing of Solid Wood with Knots. *ACM Trans. Graph.* 41, 4, Article 45 (July 2022), 9 pages. <https://doi.org/10.1145/3528223.3530081>

## 1 INTRODUCTION

Knots are commonly seen on wooden surfaces, including structural building members, wall panelling, flooring, and table tops. Knots are caused by branches growing out from the stem of the tree, which leave traces inside the wood. They cause complex distortions to the otherwise relatively straight stem grain, giving rise to distinctive annual ring patterns. Depending on the direction in which the knot faces the surface, its appearance changes from a circular spot to a curved cone (Fig. 2). Moreover, during the lifetime of a tree, a branch might die, which affects the shape of the knot and its impact on the stem grain. Knots are particularly characteristic of softwood, which is wood from conifer trees (e.g., pine and spruce). Such trees typically have many branches growing out from their main stem, giving rise to dense knot patterns in the wood texture. Nonetheless, hardwoods (e.g., oak) often have knots in their textures as well.

The level set method was successfully applied to model annual ring patterns by simulating the gradual expansion of trees [Kratt

et al. 2015; Mann et al. 2006; Sellier et al. 2011]. Although this method is suitable for handling complex geometries including grafting points and dying knots, as a growth model that evolves over many time steps and necessitates calculating and storing every point in the tree at a given resolution, it is computationally inefficient for surface texturing. Conversely, procedural texturing calculates only the points of interest (the visible pixels on the surface of the object being rendered) and does so on demand (during rendering) without storing all pixel colors as a volumetric raster image in the texture memory, making it computationally efficient and therefore a popular method for modeling volumetric materials including wood [Gardner 1984, 1985; Peachey 1985]. Previous research on procedural modeling of wood have successfully reproduced features such as rays and pores [Liu et al. 2016]. However, knots have yet to receive significant attention.

Therefore, we propose a method to procedurally model the volumetric annual ring pattern of knotted wood. The texture is structured around a grafted skeleton and we consider both alive and dead knots. We encode the internal and external geometries of an input tree log geometry in a series of image maps. By referring to these images, we calculate scalar fields of time (distance divided by the local speed of growth) around each strand of the internal grafted skeleton. The time fields are then merged using smooth minimums. Up to this point, our procedure is similar to previous methods developed for tree modeling and layered solid models in general [Cutler et al. 2002; Perlin 1985; Pirk et al. 2012]. However, we go further in modeling the details of the stem-to-knot unions. Specifically, we suggest techniques for fine-tuning the balance of smoothness and for handling dead knots, including smoothness inversion and butterfly distortions, mimicking patterns observed in real wood. The final output image is rendered by converting the time field values into pixel colors by sampling a wood color map.

To illustrate the feasibility of our method, we implemented a shader program running on a graphics processing unit (GPU) and produce a number of rendered images. For the images presented in this paper, the computation times were typically less than 1 s and the typical texture memory data size for a tree log geometry and wood colors was 600 KB, demonstrating the time- and space-efficiency of our method. We present a variety of solid wood textures with knots from pine and spruce. By modifying the texture coordinates of the input 3D model, we also reproduce the appearance of processed wood materials, specifically plywood and cross-laminated timber (CLT). The visual quality of our results were evaluated by asking wood experts to rate and comment on the plausibility of the annual ring patterns in a number of rendered images.

Finally, for possible applications, knotted wood textures is of particular interest for creating computer visualizations of architecture and furniture designs. Potential industrial applications also exists.

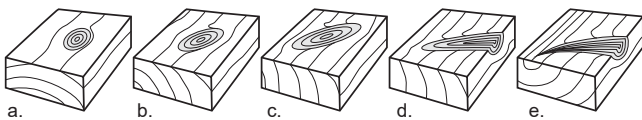


Fig. 2. Knot in various cuts [Forest Products Laboratory - USDA 2010].

For example, our model makes it possible to visualize virtually cut planks based on skeleton data extracted from computed tomography (CT) scans of tree logs, which can facilitate the selection of logs at a wood mill.

## 2 RELATED WORK

### 2.1 Texture synthesis

A popular approach to producing high-quality texture images is texture synthesis. Texture synthesis methods take a small exemplar image as input and produce similar looking texture images of arbitrary sizes. Both 2D and 3D texture synthesis methods have been proposed for wood textures [Henzler et al. 2020; Kopf et al. 2007]. A limitation with texture synthesis methods is memory efficiency. They store the synthesis result as a raster image, which requires significant memory to represent a large 3D volume, such as that of a tree log. As a more critical limitation, standard texture synthesis methods look at local features only. Although these models tend to work well for uniform materials like gravel, they fail to reconstruct global structures like the internal grafted skeleton of knotted wood. In another study, multiple texture patches were placed to model anisotropic materials, including wood [Takayama et al. 2008]. However, with this patch-based approach, the annual rings become discontinuous around boundaries of neighboring patches. Another work on macrostructured texture synthesis distributes particles on a surface with 2D texture coordinates, modelling knots as circular spots [Dischler and Ghazanfarpour 1999]. Whereas this method is arguably sufficient for recreating the appearance of knots that are cut in the traversal plane (Fig. 2a), it cannot recreate the appearance of knots that are cut other directions (Fig. 2b-e), for which it would be necessary to model their volumetric structure.

### 2.2 Procedural modeling and texturing

Procedural texturing is already a widely used technique for texturing solid wood. State-of-art research handles rays and pores as well as complex features caused by waving or spiraling behaviours of specific hardwood species and considers fiber directions, whereas knots and splits remain as open topics of future work [Liu et al. 2016; Marschner et al. 2005]. There are also several node-based editors for procedural textures, such as Blender, that allow for interactive editing of volumetric effects. Using such tools, knots would typically be modelled by randomly distributing dots inside a standard wood texture, and then adding deformations around them by noise or offsetting. However, without organizing the texture around an internal grafted skeleton, the relationship between the knots and the stem is incorrect, e.g., the knots start growing anywhere rather than at the pith (the central core of the stem skeleton). This limitation would be particularly obvious when the wood is cut at or near the pith, where the grafting point is revealed (Fig. 2e).

For materials and shapes other than wood, distance fields and smooth minimums have been used for procedural texturing and implicit modeling in general. Some research has proposed the use of 3D distance fields for procedural texturing [Oliveira et al. 2010]. Others have used 2D distance fields with smooth minimums to create abstract patterns [Ehren Choy 2016]. Another study proposed a general framework for the procedural modeling of layered solid

models including the minimum unions of solids [Cutler et al. 2002]. Furthermore, the smooth minimum is commonly used for the implicit geometry modeling of surfaces [Angles et al. 2017; Gourmel et al. 2013; Quilez 2013]. The originality of our method compared to these approaches is its application to volumetric knotted wood as well as the specific techniques we propose to control the smooth minimum to reproduce the observed effects.

### 2.3 Tree growth simulation

The growth of trees is divided into primary and secondary systems, referred to as *apical* and *cambial* growth, respectively. Apical growth elongates the tree and produces new strands of branches in various directions. This type of growth is often modeled using L-systems or the deformation of an input skeleton [Ijiri et al. 2006; Lam and King 2005; Lindenmayer 1968; Pirk et al. 2012]. Cambial growth adds a layer of new material over the entire exterior surface of the tree each year. This mode of growth is the main area of interest for this paper, because the annual expansion in thickness gives rise to the annual ring pattern. Previous studies have modeled cambial growth using the level set method to simulate the annual expansion of a tree based on various local conditions, such as sunlight, nutrition, and the presence of obstacles [Kratt et al. 2015; Mann et al. 2006; Sellier et al. 2011]. These models handle complex and multi-stranded tree skeletons, including knots. Mann et al. even considered dead knots [Mann et al. 2006]. However, the level set method is a growth model where the shape expands over many time steps, and thus it tends to be computationally expensive.

## 3 OBSERVATIONS

A knot starts growing from the pith of the stem and has a more or less pronounced curvature pointing up or down. The speed of growth of the volume expansion (added yearly thickness) is higher for the stem than the knots, resulting in denser annual rings inside the knots in comparison to the stem. In the presence of knots, the stem grain is distorted when the fibers of the stem are forced to deviate from their otherwise relatively vertical path. Moreover, at a given point, a knot is alive or dead, which affects its appearance and distortion effect (Fig. 3).

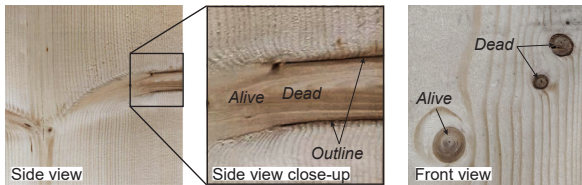


Fig. 3. Photographs of pine wood with knots.

### 3.1 Alive knots

An alive knot is intergrown with the stem, i.e., the stem grain flows into the knot and becomes a part of it. The radius of the fillet of the stem-to-knot transition gradually increases over time; at an older age close to the pith of the tree, the radius is smaller, and at a younger age, the radius is larger [Foley 2003]. Moreover, knots have a darker color than the stem grain.

### 3.2 Dead knots

After a branch dies, it stops growing in thickness. A dead knot is no longer intergrown, and the deformation effect on the surrounding grain decreases. Close to the edge of the knot, the smoothness tends to invert, i.e., starts pointing inward toward the pith of the tree. Moreover, butterfly patterns occasionally appear around recently dead knots. To understand the internal geometry that causes these patterns, we CT scanned samples of wood (Fig. 4). The scans show that the grain deformation is stronger above and below the knot compared to the sides. We therefore conclude that butterfly patterns are caused by a nonuniform deformation around the axis of the knot. Moreover, a dead knot darkens over time, and takes an outline.

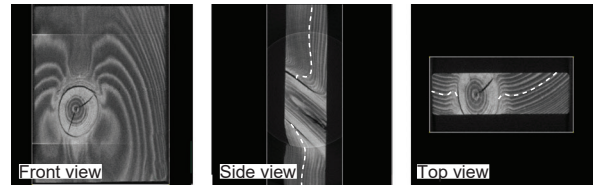


Fig. 4. CT-scan images of a wood sample with a butterfly distortion pattern.

## 4 METHOD AND IMPLEMENTATION

The proposed method takes a 3D surface model as well as the internal and external geometry of a tree log as inputs and renders the 3D model with a knotted wood grain texture (Fig. 5). The procedure first calculates the time fields around each strand, i.e., the stem and each knot (Sec. 4.1). Second, the time fields are combined using smooth minimums while considering whether each knot is alive or dead at the given point in time (Sec. 4.2). Third, the time values are translated into wood colors by sampling a wood color map and additionally darkening the knots (Sec. 4.3). Finally, we present the input tree log data and how they are encoded into images (Sec. 4.4). The process was written in OpenGL Shading Language (GLSL) using less than 500 lines of code of the fragment shader, in which the procedure is executed. The Phong lighting model was used for illumination [Phong 1975].

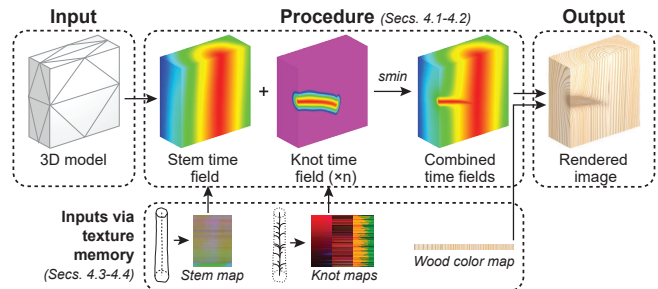


Fig. 5. Overview of the proposed system.

#### 4.1 Representation of annual rings

We define the volumetric texture of the wood grain using a 3D scalar field representing the time when the growth occurred, which we refer to as a *time field* (Fig. 6). A tree grows from the center outwards, and thus the time value is 0.0 along the pith of the tree, and 1.0 on the exterior surface. An annual ring between can be seen as an isocurve of the time field, i.e., a curve implicitly defined by a constant value (e.g., 0.4). The magnitude of the gradient (or distance between annual rings) varies with the speed of the growth.

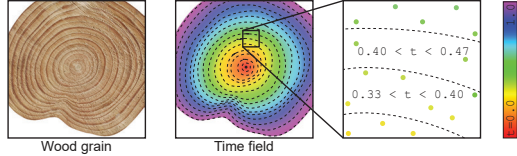


Fig. 6. Time field representation of wood grain.

**4.1.1 Time field calculation.** Time values are first calculated separately for each skeleton strand as the distance to the strand divided by the speed of growth in the current direction. Or, in other words, given the world coordinates of a point ( $P \in \mathbb{R}^3$ ) on a 3D model, the time value ( $t$ ) for a skeleton strand is defined by

$$t = \frac{\text{dist}(S, P)}{v(S, \beta)} \quad (1)$$

where  $S \in \mathbb{R}^3$  is the point on the strand nearest to  $P$ , and  $v(S, \beta)$  is the speed of growth at point  $S$  on the strand in the orientation  $\beta$  of  $P$  around the strand.

Exact computation of the closest point  $S$  is costly. Therefore, we apply a simplification to take a pseudo-nearest point. For the stem, we define the pseudo-nearest point as the point on the stem skeleton with equal height ( $z$ ) as  $P$ . For knots, the pseudo-nearest point on the branch skeleton is the point at an equal distance ( $d$ ) from the stem as  $P$ . Variation of the speed of growth is defined explicitly for the stem through the outer shape of the input tree log geometry (see Sec. 4.4). The speed of growth of the knots is set to a fraction of the speed for the stem and, additionally, a variation is created inside the procedure using periodic Perlin noise [Perlin 1985, 2002].

#### 4.2 Stem-to-knot transition

The smooth minimum is commonly used to create unions with a continuous seam between implicitly defined surfaces (Fig. 7, left). When applied to time field volumes, it creates a continuous seam between each layer (Fig. 7, right).

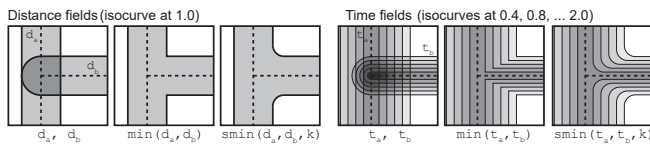


Fig. 7. Minimums and smooth minimums of distance and time fields.

There are several established functions for smooth minimum unions, including *exponential*, *polynomial*, and *power* smooth minimums, which result in different shapes of the fillets (Fig. 8) [Quilez 2013]. Among these, we use the power smooth minimum for two reasons. First, there are no artifacts caused by negative values at the skeleton grafting points, unlike for the exponential and polynomial smooth minimums. Second, with the power smooth minimum, the smoothness naturally increases over time, i.e., the radius of the union is smaller closer to the pith and larger further out in the tree, which is consistent with behaviour observed in real wood (see Sec. 3.1).

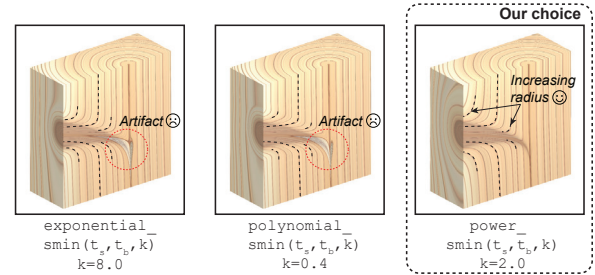


Fig. 8. Results of different smooth minimum functions.

The equation of the power smooth minimum function  $smin$  is

$$smin(t_a, t_b, k) = \left( \frac{t_a^k t_b^k}{t_a^k + t_b^k} \right)^{\frac{1}{k}} \quad [\text{Quilez 2013}] \quad (2)$$

where  $t_a$  and  $t_b$  are scalar values at a point in the field, and  $k$  is a parameter that controls the degree of smoothness. A smaller  $k$  results in a softer union, whereas a larger value creates a sharper union. We introduce a technique to fine-tune the shape of the smooth union by adapting the parameter value ( $k$ ) within a field (see Sec. 4.2.1). Furthermore, we refer to the difference between the smooth minimum and minimum as the *amount of smoothing* ( $\delta$ ):

$$\delta = smin(t_a, t_b, k) - \min(t_a, t_b) \quad (3)$$

This value ( $\delta$ ) is useful for the analytical purpose of visualizing the amount of smoothing (e.g., red gradient in Fig. 9). Moreover, we introduce a second technique to adjust the shape of the smooth minimum by modifying  $\delta$ :

$$smin'(t_a, t_b, k) = \min(t_a, t_b) + \delta' \quad (4)$$

In particular, we use this technique for controlling the direction of the grain distortion around a dead knot (see Sec. 4.2.2). We also use the amount of smoothing ( $\delta$ ) to handle many knots with individual smoothness properties in a single texture (see Sec. 4.2.3).

**4.2.1 Modelling an alive knot.** When joining the time fields of a knot and the stem by the power smooth minimum, it naturally creates the appearance of an alive knot: the thickness of the knot increases with time and the knot is intergrown with the stem. However, we want to adjust the balance of smoothness to create a sharper edge of the knot without reducing its distortion effect in the stem. This is achieved by an adaptive  $k$ -value; we set a higher  $k_b$  inside the knot (for a tighter edge) and a lower  $k_s$  outside the knot (for a stronger

distortion effect). We create a smooth transition between these two  $k$ -targets based on the variable  $t_{\Delta}$ , which is the signed difference between the time values of the stem ( $t_s$ ) and knot ( $t_b$ ). The result is a more defined knot edge with a maintained distortion effect compared to a constant  $k$  (Fig. 9).

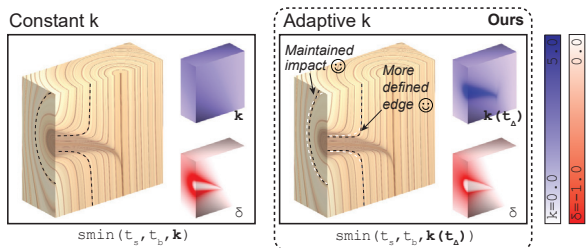


Fig. 9. An adaptive  $k$ -value (right) creates a more defined knot edge with maintained distortion impact, in comparison to a constant  $k$ -value (left).

**4.2.2 Modelling a dead knot.** To make a knot stop growing in thickness from when it dies ( $t_{\dagger}$ ), the expansion of the knot is gradually decreased from this point onward to counteract the natural increase in thickness (Fig. 10). Furthermore, we want to control the fillet around a dead knot such that the overall distortion effect decreases and the direction of the fillet changes close to the edge of the knot. By adjusting the parameter  $k$ , it is possible to increase or decrease the smoothing effect, but not to invert it. Thus, another technique is required. Building on Eq. 4, the amount of smoothing ( $\delta$ ) is modified by scaling it by a factor  $f$ . When scaled by a negative value, the smoothness inverts. The factor  $f$  is calculated as a function of two variables: time since death ( $t_{\dagger\Delta}$ ) and orientation around the knot axis ( $\beta$ ). The time since death ( $t_{\dagger\Delta}$ ) is used as a variable to gradually change the direction of the smoothness with increased distance from the point of death. The orientation ( $\beta$ ) is used to create a non-uniform deformation around the knot axis to produce a butterfly pattern.

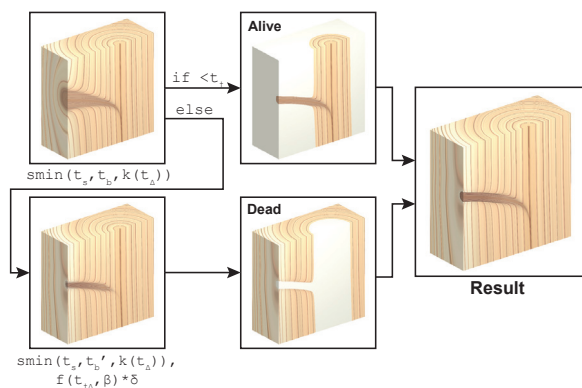


Fig. 10. Modelling a dead knot.

The value of interest for the next step in the calculation (joining multiple knots to the stem, Sec. 4.2.3) is the modified amount of

smoothing ( $\delta'$ ), the complete calculation of which is summarized as

$$\delta' = \begin{cases} \text{smmin}(t_s, t_b, k(t_{\Delta})) - \text{min}(t_s, t_b), & \text{if alive} \\ f(t_{\dagger\Delta}, \beta) \cdot (\text{smmin}(t_s, t'_b, k(t_{\Delta})) - \text{min}(t_s, t'_b)), & \text{otherwise} \end{cases} \quad (5)$$

**4.2.3 Multiple knots.** Finally, we want to merge multiple knots to the stem. It is possible to extend the equation of the power smooth minimum to perform a union between more than two fields at once [Quilez 2013]. However, this is problematic in our case because it does not allow us to control the smoothness individually for each knot. Sequential smooth minimums are also problematic because the order matters. Our solution is to calculate the modified smoothing value ( $\delta'_i$ ) for each pairwise  $i$ -th knot and stem union separately, as shown in Eq. 5 and add their sum to the regular minimum of all knots (Fig. 11):

$$\text{smmin}'(t_s, t_{b_1}, \dots, t_{b_n}) = \text{min}(t_s, t_{b_1}, \dots, t_{b_n}) + \sum_{i=1}^n \delta'_i \quad (6)$$

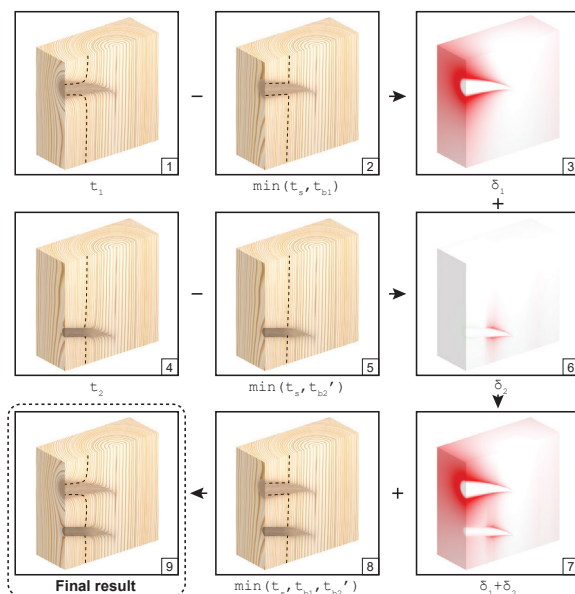


Fig. 11. Joining the stem and multiple knots (Eq. 6).

### 4.3 Color rendering

To translate the time field into wood colors, we map it to a one-dimensional wood color map, i.e., an array of pixels. The wood color map contains color information ranging from the pith to the outer surface of the tree. It can be sampled from a picture of a stem (Fig. 12), procedurally synthesized (using a separate process), or manually designed using photo editing software. Furthermore, the color of the knots are darkened during the procedure by subtracting an arbitrary color inside the knots. In addition, we add an outline around a dead knot, the thickness of which is varied with periodic Perlin noise for a natural appearance.

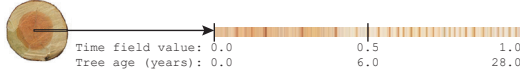


Fig. 12. Wood color map.

#### 4.4 Input tree log data

The input tree log data consist of its internal grafting skeleton, its outer surface, and the point of dying of each knot. These data are encoded in image files, which are uploaded to the texture memory and sampled during the procedure. An advantage of using an input geometry instead of generating it inside the procedure is portability (saving instances of trees). This setup allows feeding data that have been extracted from CT-scan slices of tree logs as input into the procedure. The main benefits of encoding the geometry in images as opposed to text files, for example, are compactness and visual verification. To avoid aliasing, the value ranges are kept as narrow as possible and the image maps are sampled with a bi-cubic function. The total size of the four image maps describing the input geometry is approximately 400 KB in our current implementation (excluding 200 KB for the wood color data).

**4.4.1 Stem geometry.** The skeleton strand and outer surface of the stem are encoded in an image, referred to as the *stem map* (Table 1 and Fig. 13). The horizontal image axis corresponds to the orientation around the tree ( $\omega$ ), and the vertical axis corresponds to the height inside the tree ( $z$ ). The pixel values encode the x- and y-coordinates of the pith point, and the local stem radius. The pith point varies with height ( $z$ ) but is constant along each row (the rotation around the tree does not change the pith point), whereas the local radius varies with the height ( $z$ ) and orientation ( $\omega$ ). The proposed data structure is based on research documenting CT-scanned timber logs [Grönlund et al. 1995]. We currently use an RGB texture image with a pixel resolution of  $128 \times 512$  for the stem geometry.

Table 1. Geometric data encoded in the stem map.

Image		Data	Range
Axis	X	Rotation ( $\omega$ )	0.0 to $2\pi$
	Y	Height ( $z$ )	0.0 to $h$
Color	R	Pith point x ( $S_x$ )	$-0.5 \cdot r_{smin}$ to $0.5 \cdot r_{smin}$
	G	Pith point y ( $S_y$ )	$-0.5 \cdot r_{smin}$ to $0.5 \cdot r_{smin}$
	B	Radius ( $r_s$ )	$r_{smin}$ to $r_{smax}$

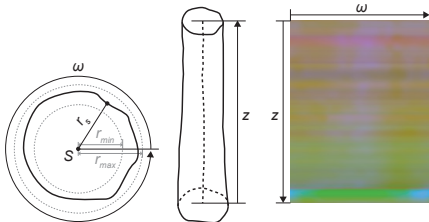


Fig. 13. Tree stem geometry and stem map.

**4.4.2 Knot geometries.** We encode the geometries of the knots in three image maps: the *knot height*, *knot orientation*, and *knot state maps* (Table 2 and Fig. 14). For these maps, the horizontal image axis corresponds to the distance from the pith ( $d$ ), and the vertical image axis to the knot index. For a particular knot index and distance from the pith, the knot skeleton point is given by its height in the tree ( $z$ ) and orientation around the vertical axis ( $\omega$ ), which are sampled from the *knot height* and *knot orientation maps*, respectively. Both the height and orientation values change with distance from the pith as the height-wise curvature and rotational twist of the knot progress (Fig. 14). The third map—the *knot state map*—indicates when the knot is alive or dead. This data structure used to describe the knots builds on knot formulas developed by Grönlund et al. and refined by Andreu et al. and Johansson et al. to document structural timber [Andreu and Rinnhofer 2003; Grönlund et al. 1995; Johansson et al. 2013]. We currently use three RGB images with a pixel resolution of  $32 \times 256$  for the knot geometries.

Table 2. Geometric data encoded in the three knot maps.

Image		Data	Range
All	Axis	X	Pith distance ( $d$ )
		Y	Knot index
<i>Knot height map</i>	Color	R	Start ( $z_0$ )
		G	Increase ( $z_+$ )
		B	Decrease ( $z_-$ )
<i>Knot orientation map</i>	Color	R	Start ( $\omega_0$ )
		G	Left ( $\omega_{ccw}$ )
		B	Right ( $\omega_{cw}$ )
<i>Knot state map</i>	Color	R	Alive
		G	Time of death ( $t_+$ )

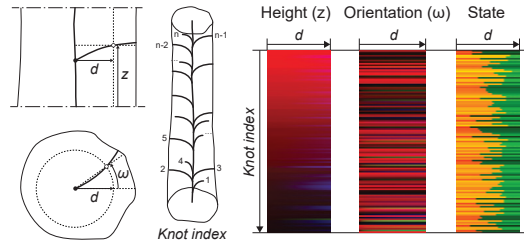


Fig. 14. Knot geometries and knot maps.

## 5 RESULTS

Our results consist of rendered images. First, we show different cut-outs of the same tree geometry (Fig. 15). This result demonstrates that, unlike previous texturing methods that distribute circular knots spot-wise on a surface based on 2D texture coordinates [Dischler and Ghazanfarpour 1999], our method recreates the appearance of knots that are cut along their skeletons, and thus have a curved conical profile. In another result, to demonstrate the expressiveness of our model, we rendered the same cut-out with randomized knot skeletons and parameters (Fig. 16). This shows that diverse shapes

and sizes of knots emerge by varying their curvatures and positions, as well as speed of growth and time of death. Moreover, to show that our method efficiently handles many and diverse knots in a texture that spans over a larger portion of a tree, we also present long planks. These were rendered based on captured data extracted from CT-scan slices from pine and spruce.<sup>1</sup> Furthermore, we present four rendered images aimed at reproducing the grain patterns and colors of reference photographs (Fig. 1). Specifically, we reconstructed a) wood with longitudinal cut through a knot transitioning from alive to dead, b) a butterfly pattern around a dead knot, c) a knot located at the boarder between the heart- and sapwood, and d) a typical grouping pattern of multiple knots. For these rendered images, the wood color maps were created using a separate small program that exports a 1D wood grain pattern based on sample colors. We loaded the captured data from a pine tree and manually searched for a good position inside the tree. We occasionally changed the geometrical data manually, such as the angular position of a knot, to better match the reference image.

Finally, we show that our method can easily be extended for representing common softwood products, namely CLT and plywood. To produce these textures, we use the same pine tree geometry as in Fig. 17a, but manipulate the input texture coordinates. First, for CLT, the texture coordinates were offset and rotated orthogonality to achieve a tiling effect (Fig. 18a). We also added noise to the colors to achieve a contrast between neighboring planks. Second, plywood (and also wood veneer) is manufactured through the rotational cutting of a tree log. Therefore, to recreate the plywood texture, the texture coordinates of the input 3D model were unrolled in a corresponding manner (Fig. 18b).

The typical computation time for the rendered images presented in this paper was under 1 s, using a texture memory of up to 600 KB. All images were rendered using a laptop computer with a 1.3 GHz CPU and GPUs of 15.8 and 19.8 GB.

## 6 EVALUATION

Our results were qualitatively evaluated by 10 wood experts from academia (80%) and industry (20%). Their expertise include timber grading, timber log scanning, mechanics of wood, as well as image analysis of wood. Using an online questionnaire, we asked them to rate and comment on the plausibility of the annual ring patterns in four rendered still images (Figs. 1a, 1b, 1d, and 17b). Although explicitly asked to comment on the shape of the annual ring pattern, which is the primary focus of the current work, the experts often mentioned colors in their answers. The average rating was 3.8 out of 5 (1 = strongly disagree, 5 = strongly agree). The most highly rated (4.0/5) image is shown in Fig. 1d. Expert 7 commented that the annual ring pattern appears to be correct, while the knot color is too dark. The second highest rated (3.9/5) rendered image is shown in Fig. 1a. Expert 5 stated that this image shows a “*very realistic transition from a sound [alive] to dead knot.*” The third highest rated (3.7/5) image was the butterfly pattern shown in Fig. 1b. Expert 3 stated that “*one of the butterfly wings should be a little larger than the other,*” whereas Expert 5 thought the distortion looked too regular.

<sup>1</sup>We received this data directly from the computed tomography (CT) laboratory, division of Wood Science and Technology, Luleå Technical University, Sweden.



Fig. 15. Rendered images of different portions of a tree with constant parameters and knot skeleton



Fig. 16. Rendered images of same portion of a tree, with randomized parameters and knot skeletons (same wood color map).

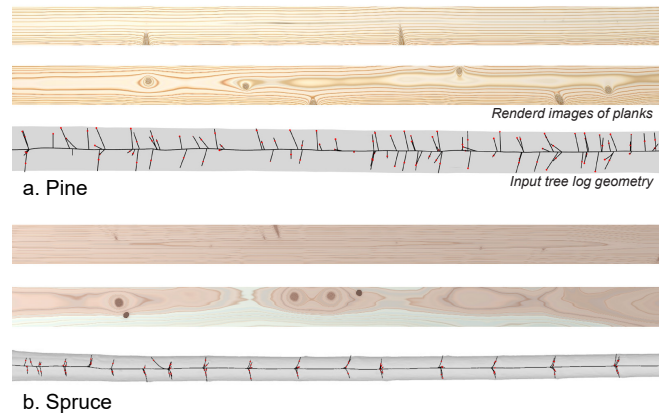


Fig. 17. Rendered images of planks and their corresponding input tree log geometries that have been extracted from CT-scan data.

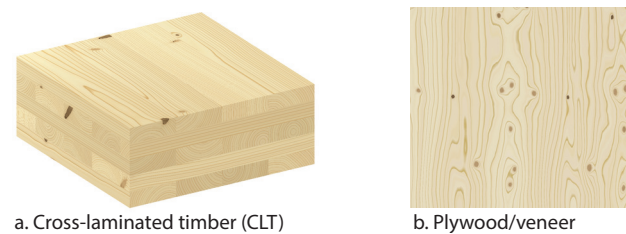


Fig. 18. Rendered images of softwood products.

The lowest rated (3.4/5) set of images was the spruce planks shown in Fig. 17b, for which the experts cited an excessively light color of the sapwood and an overly dark color of the knots. In summary, the experts found the modelled annual ring patterns plausible. They indicated that the results could be improved applying more noise to

the distortions, especially around the knots. It was further suggested that the coloring need more fine-tuning. Refer to the supplementary materials for the complete questionnaire and answers.

## 7 LIMITATIONS AND FUTURE WORK

The limitations of our model are as follows. Branches can naturally fall off or be pruned. It is non-trivial to make the breaking off point look natural inside the wood texture and thus we left this for future work. Moreover, our current model cannot selectively change the growth speed at an arbitrary year of an arbitrary height or angle. Related to this limitation, the wood grain colors and number of year rings do not change with height in our model, whereas in reality, the top of a tree will have fewer annual rings and a larger proportion of sapwood to heartwood in comparison to the bottom of a tree. Furthermore, it is possible to add various features to make the results of our function appear more like real wood, including cracks, rays, pores, fiber directions, as well as more high-frequency detail in the annual ring pattern. Also, our model does not currently include a reflectance model (BRDF).

A general drawback of procedural models is that the visual result of editing parameters is hard to predict. The results presented in this paper are produced by the authors who have developed an intuition for how to edit the parameters to achieve desired effects, making the process of designing a texture rather effortless. It would be more challenging for a novice user to reconstruct a knotted wood texture with a specific intention. For such users, a parameter overview in Appendix A is useful as a guide. Also, the almost instant rendering time facilitates the trial and error process. Nonetheless, future work might extend our method with an interface that enables more intuitive texture design. Another direction for future work is to use our modelling framework as a basis for the simulation of the mechanical properties of knotted wood.

## ACKNOWLEDGMENTS

This work was supported by a collaborative research fund between Mercari Inc. R4D and RIISE, University of Tokyo, JST ACT-X Grant Number JPMJAX210P, Japan, JST CREST Grant Number JPMJCR17A1, Japan, and JST ACT-I Grant Number JPMJPR17UT, Japan. We would further like to thank the anonymous reviewers and the participants of the expert evaluation for their constructive feedback.

## REFERENCES

- Jean Philippe Andreu and Alfred Rinnhofer. 2003. Modeling knot geometry in norway spruce from industrial CT images. *Lecture Notes in Computer Science (including subseries Lecture Notes in Artificial Intelligence and Lecture Notes in Bioinformatics)* 2749 (2003). [https://doi.org/10.1007/3-540-45103-x\\_{1}104](https://doi.org/10.1007/3-540-45103-x_{1}104)
- Baptiste Angles, Marco Tarini, Brian Wyvill, Loïc Barthe, and Andrea Tagliasacchi. 2017. Sketch-based implicit blending. In *ACM Transactions on Graphics*, Vol. 36. <https://doi.org/10.1145/3130800.3130825>
- Barbara Cutler, Julie Dorsey, Leonard McMillan, Matthias Müller, and Robert Jagnow. 2002. A procedural approach to authoring solid models. In *Proceedings of the 29th Annual Conference on Computer Graphics and Interactive Techniques, SIGGRAPH '02*. <https://doi.org/10.1145/566570.566581>
- Jean Michel Dischler and Djamchid Ghazanfarpour. 1999. Interactive image-based modeling of macrostructured textures. *IEEE Computer Graphics and Applications* 19, 1 (1999). <https://doi.org/10.1109/38.736470>
- Ehren Choy. 2016. *Smooth Signed Distance Field Textures*. Ph.D. Dissertation. Carleton University, Ottawa.
- Christina Foley. 2003. *Modeling the effects of knots in Structural Timber*. Ph.D. Dissertation. Lund University. <https://lup.lub.lu.se/search/publication/f026a551-2812-4539-98a2-0e7ee2ca4d5f>
- Forest Products Laboratory - USDA. 2010. *Wood Handbook: Wood as an Engineering Material*.
- Geoffrey Y. Gardner. 1984. SIMULATION OF NATURAL SCENES USING TEXTURED QUADRIC SURFACES. *Computer Graphics (ACM)* 18, 3 (1984). <https://doi.org/10.1145/964965.808572>
- Geoffrey Y. Gardner. 1985. VISUAL SIMULATION OF CLOUDS. *Computer Graphics (ACM)* 19, 3 (1985). <https://doi.org/10.1145/325165.325248>
- Olivier Gourmel, Loïc Barthe, Marie Paule Cani, Brian Wyvill, Adrien Bernhardt, Mathias Paulin, and Herbert Grasberger. 2013. A gradient-based implicit blend. *ACM Transactions on Graphics* 32, 2 (2013). <https://doi.org/10.1145/2451236.2451238>
- Anders Grönlund, Lars Björklund, Stig Grundberg, and Göran Berggren. 1995. *Manual för furustambank*. Technical Report. Luleå Technical University.
- Philipp Henzler, Niloy J. Mitra, and Tobias Ritschel. 2020. Learning a Neural 3D Texture Space from 2D Exemplars. In *Proceedings of the IEEE Computer Society Conference on Computer Vision and Pattern Recognition*. IEEE Computer Society, 8353–8361. <https://doi.org/10.1109/CVPR4260.2020.00838>
- Takashi Ijiri, Shigeru Owada, and Takeo Igarashi. 2006. The sketch L-system: Global control of tree modeling using free-form strokes. In *Lecture Notes in Computer Science (including subseries Lecture Notes in Artificial Intelligence and Lecture Notes in Bioinformatics)*, Vol. 4073 LNCS. [https://doi.org/10.1007/11795018\\_{1}13](https://doi.org/10.1007/11795018_{1}13)
- Erik Johansson, Dennis Johansson, Johan Skog, and Magnus Fredriksson. 2013. Automated knot detection for high speed computed tomography on *Pinus sylvestris* L. and *Picea abies* (L.) Karst. using ellipse fitting in concentric surfaces. *Computers and Electronics in Agriculture* (2013). <https://doi.org/10.1016/j.compag.2013.06.003>
- Johannes Kopf, Chi Wing Fu, Daniel Cohen-Or, Oliver Deussen, Dani Lischinski, and Tien Tsin Wong. 2007. Solid texture synthesis from 2D exemplars. *ACM Transactions on Graphics* (2007). <https://doi.org/10.1145/1276377.1276380>
- J. Kratt, M. Spicker, A. Guayaquil, M. Fiser, S. Pirk, O. Deussen, J. C. Hart, and B. Benes. 2015. Woodification: User-Controlled Cambial Growth Modeling. In *Computer Graphics Forum*, Vol. 34. <https://doi.org/10.1111/cgf.12566>
- Z. Lam and Scott A. King. 2005. Simulating tree growth based on internal and environmental factors. In *Proceedings - GRAPHITE 2005 - 3rd International Conference on Computer Graphics and Interactive Techniques in Australasia and Southeast Asia*. <https://doi.org/10.1145/1101389.1101406>
- Aristid Lindenmayer. 1968. Mathematical models for cellular interactions in development I. Filaments with one-sided inputs. *Journal of Theoretical Biology* 18, 3 (1968). [https://doi.org/10.1016/0022-5193\(68\)90079-9](https://doi.org/10.1016/0022-5193(68)90079-9)
- Albert Julius Liu, Zhao Dong, Miloš Hašan, and Steve Marschner. 2016. Simulating the structure and texture of solid wood. *ACM Transactions on Graphics* (2016). <https://doi.org/10.1145/2980179.2980255>
- Joanne Mann, Mike Plank, and Andy Wilkins. 2006. Tree growth and wood formation — applications of anisotropic surface growth. In *Proceedings of the Mathematics in Industry Study Group*. 153–192.
- Stephen R. Marschner, Stephen H. Westin, Adam Arbree, and Jonathan T. Moon. 2005. Measuring and modeling the appearance of finished wood. In *ACM Transactions on Graphics*. <https://doi.org/10.1145/1073204.1073254>
- Guilherme N. Oliveira, Rafael P. Torchelsen, João L.D. Comba, Marcelo Walter, and Rui Bastos. 2010. Geotextures: A multi-source geodesic distance field approach for procedural texturing of complex meshes. In *Proceedings - 23rd SIBGRAPI Conference on Graphics, Patterns and Images, SIBGRAPI 2010*. <https://doi.org/10.1109/SIBGRAPI.2010.25>
- Darwyn R. Peachey. 1985. SOLID TEXTURING OF COMPLEX SURFACES. *Computer Graphics (ACM)* 19, 3 (1985). <https://doi.org/10.1145/325165.325246>
- Ken Perlin. 1985. An Image Synthesizer. In *Proceedings of the 12th Annual Conference on Computer Graphics and Interactive Techniques (SIGGRAPH '85)*. Association for Computing Machinery, New York, NY, USA, 287–296. <https://doi.org/10.1145/325334.325247>
- Ken Perlin. 2002. Improving Noise. In *Proceedings of the 29th Annual Conference on Computer Graphics and Interactive Techniques (San Antonio, Texas) (SIGGRAPH '02)*. Association for Computing Machinery, New York, NY, USA, 681–682. <https://doi.org/10.1145/566570.566636>
- Bui Tuong Phong. 1975. Illumination for Computer Generated Pictures. *Commun. ACM* 18, 6 (1975). <https://doi.org/10.1145/360825.360839>
- Sören Pirk, Ondrej Stava, Julian Kratt, Michel Abdul Massih Said, Boris Neubert, Radomir Měch, Bedrich Benes, and Oliver Deussen. 2012. Plastic trees: Interactive self-adapting botanical tree models. *ACM Transactions on Graphics* 31, 4 (2012). <https://doi.org/10.1145/2185520.2185546>
- Inigo Quilez. 2013. Smooth minimum. <https://www.iquilezles.org/www/articles/smin/smin.htm>
- Damien Sellier, Michael J. Plank, and Jonathan J. Harrington. 2011. A mathematical framework for modelling cambial surface evolution using a level set method. *Annals of Botany* 108, 6 (2011). <https://doi.org/10.1093/aob/mcr067>
- Kenshi Takayama, Makoto Okabe, Takashi Ijiri, and Takeo Igarashi. 2008. Lapped solid textures: Filling a model with anisotropic textures. *ACM Transactions on Graphics* 27, 3 (2008). <https://doi.org/10.1145/1360612.1360652>

A PARAMETERS USED IN THE PROCEDURE

Figs. 19-22 show the effect of adjusting the various parameters. Parameters in Figs. 19a-b, 21a and 22a are controlled via the input image maps (see Secs. 4.3 and 4.4). Other parameters are scalar values that can be manually edited to achieve custom effects.

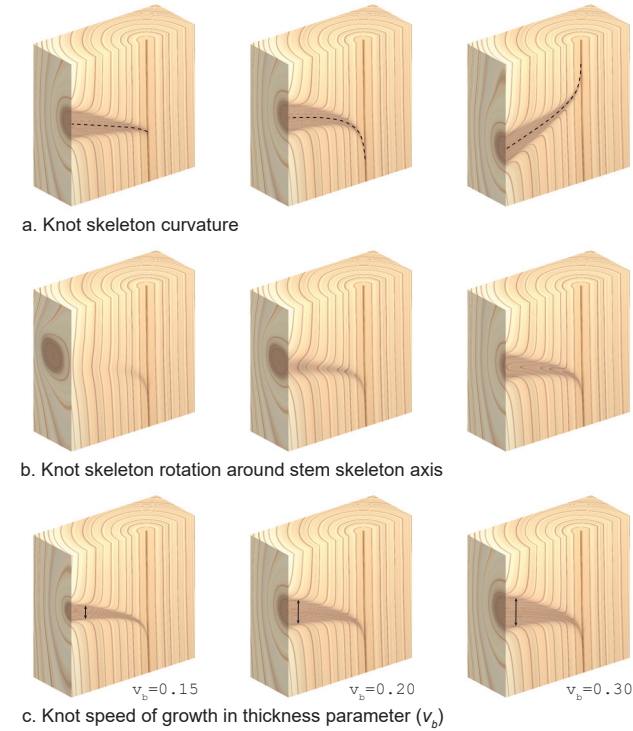


Fig. 19. Knot shape parameters.

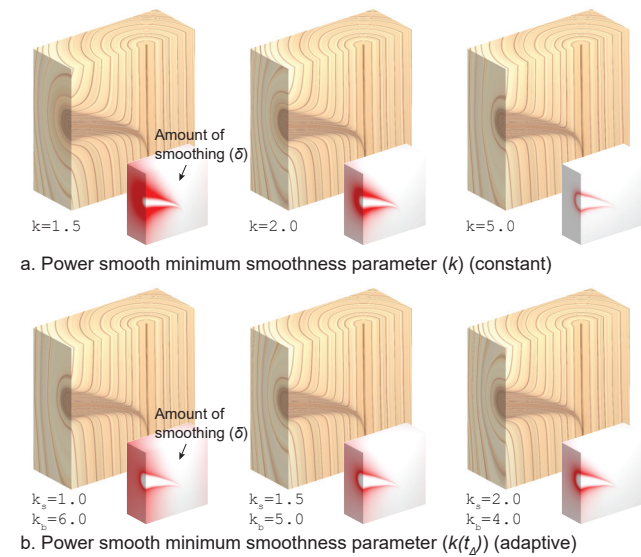


Fig. 20. Smoothness parameters.

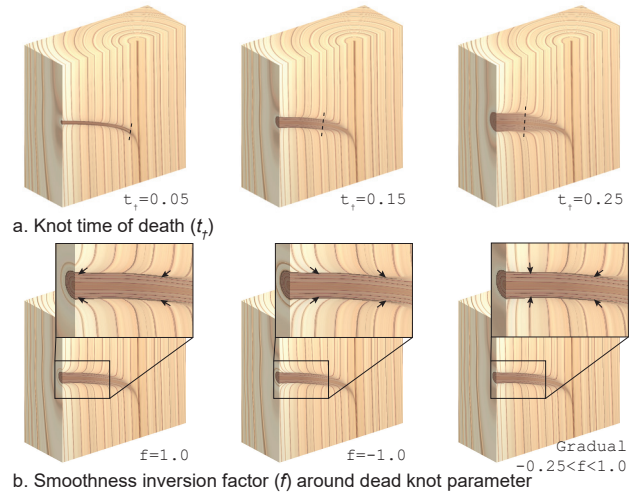


Fig. 21. Dead knot parameters.

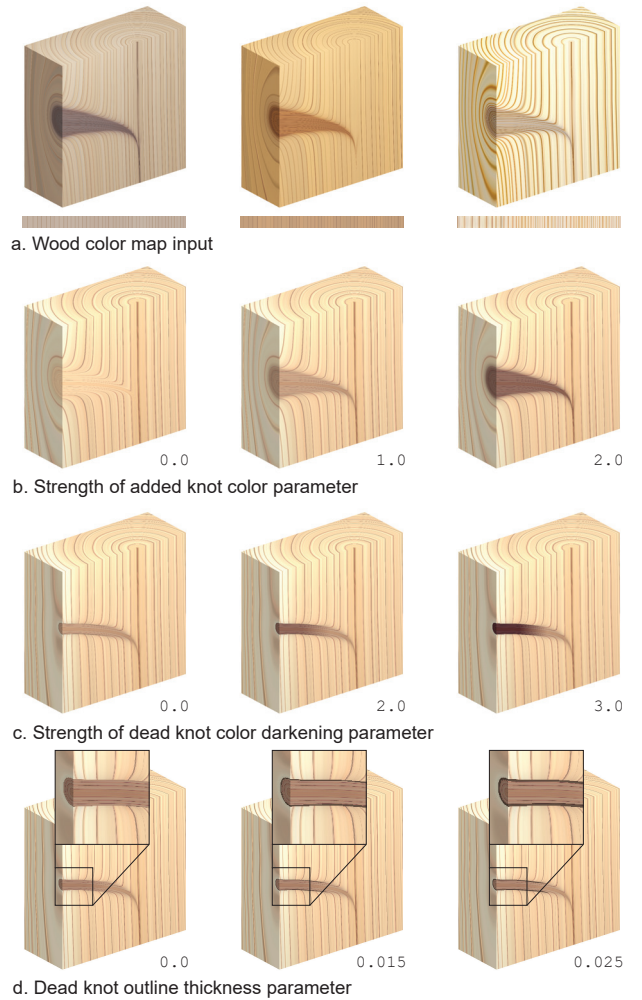


Fig. 22. Color inputs and parameters.